SURFACE FEATURES ON GLASS SPHERULES FROM THE LUNA 16 SAMPLE

JACK B. HARTUNG, FRIEDRICH HÖRZ, DAVID S. McKAY, and FRANK L. BAIAMONTE

NASA Manned Spacecraft Center, Houston, Tex., U.S.A.

Abstract. Two ellipsoidal spherules approximately 0.5 mm in diameter were studied in detail using a scanning electron microscope. A variety of surface features were observed: vesicles, mounds, dimples, streaks, ridges, grooves, accretion phenomena, and high-speed impact craters. The diameters of 27 glass-lined pits formed by impact on one spherule range from less than 1 μm to approximately 50 μm. Intermediate-sized glass-lined pits surrounded by concentric fractures demonstrate the transition between larger craters that have both a pit and a spall zone and generally smaller craters that have only a pit. Assuming all craters showing evidence of impact-related melting or flow are the result of primary impacts, the differential mass spectrum of impacting meteoroids in the range 10^{-11} to 10^{-10} g is in good agreement with a spectrum based on satellite-borne particle-detecting experiments.

1. Introduction

A variety of small-scale surface features have been described from lunar fines returned by Apollo missions 11, 12, and 14 (Carter and MacGregor, 1970; McKay, 1970; Cloud *et al.*, 1970; Frondel *et al.*, 1970; McKay *et al.*, 1970; Devaney and Evans, 1970; Neukum *et al.*, 1970; Bloch *et al.*, 1971a). These detailed morphological and chemical studies revealed surface features indicative of a variety of lunar surface processes such as melting, vaporization, condensation, exsolution of metal phases, deposition of particulate material and small-scale impact cratering. Results of similar studies of lunar material returned from Mare Fecunditatis by Luna 16 are reported here.

2. Observations

From a large number of particles investigated with an optical microscope, two glass spherules were chosen from the sample designated $\Gamma - 12$. Observations were made at magnifications of as much as 20000 times using a scanning electron microscope. Overall views of the two spherules studied are shown in Figure 1. Both spherules are ellipsoidal in shape, one being prolate and the other oblate. The longest dimensions of the spherules are 0.5 and 0.6 mm, respectively.

A. VESICLES

Very nearly spherical vesicles were observed both at the surface and inside a spherule (Figure 2). These vesicles range in size from less than 1 μm to 40 μm in diameter. They are easily distinguished from impact craters by the absence of any rim structure or fracturing. Vesicles undoubtedly were present within the spherule at the time of its formation. This suggests that the spherule did not form by condensation of a gaseous phase.

The Moon **5** (1972) 436–446.

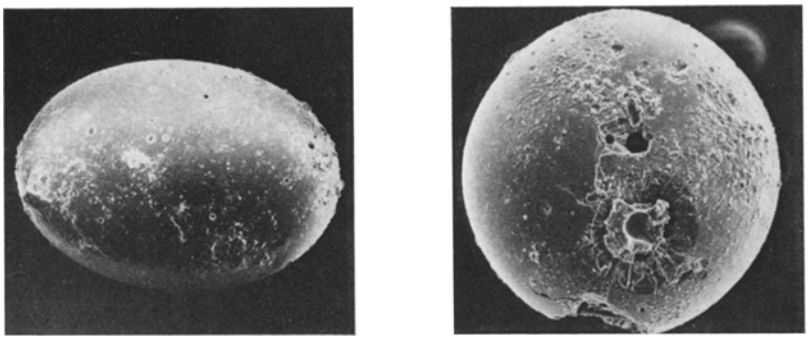

Fig. 1. Overall views of two spherules selected from the Luna 16 sample for detailed study. (a) Prolate ellipsoid displaying a variety of surface features, *e.g.* vesicles, mounds and dimples, streaks and grooves, and accretion phenomena but no obvious high-speed impact craters. (b) Oblate ellipsoid with features similar to those on the spherule in Figure 1 (a) and with a population of high-speed impact craters. The largest such crater is seen at the lower center of the view.

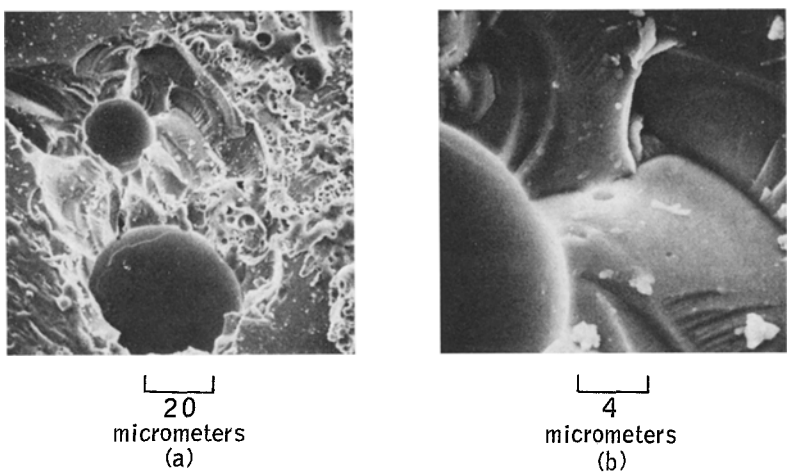

Fig. 2. Two larger interior vesicles exposed by the fracturing and removal of surface material from the spherule shown in Figure 1 (b). (a) Numerous smaller vesicles appear on the right side of the photograph, but these are related to glass splash that was apparently deposited after solidification of the spherule. (b) A detail showing the wall of a large vesicle, the fracture surfaces, and a tiny vesicle. The brighter-appearing area around the tiny vesicle is an artifact.

B. MOUNDS AND DIMPLES

On the spherule shown in Figure 1(a), isolated individual mounds and sets of roughly aligned mounds were observed (Figure 3). The lighter shade of the mound material indicates a difference in chemical composition between the mounds and the host spherule. Occurring often among the mounds are depressions or dimples that have

essentially the same diameter and that share the same alignment as the mounds. Apparently, dimples are depressions in the host spherule that once contained a mound. The mounds are shaped like thick convex-convex lenses. Similar features, where the mounds were nickel and iron, have been described from Apollo materials by Carter and MacGregor (1970).

Mounds may be produced by condensation or exsolution. The linear alignment of mounds that was observed suggests a gentle collision of small, spherical, still-molten droplets of mound material with the larger, still-plastic spherule. The cause of mound

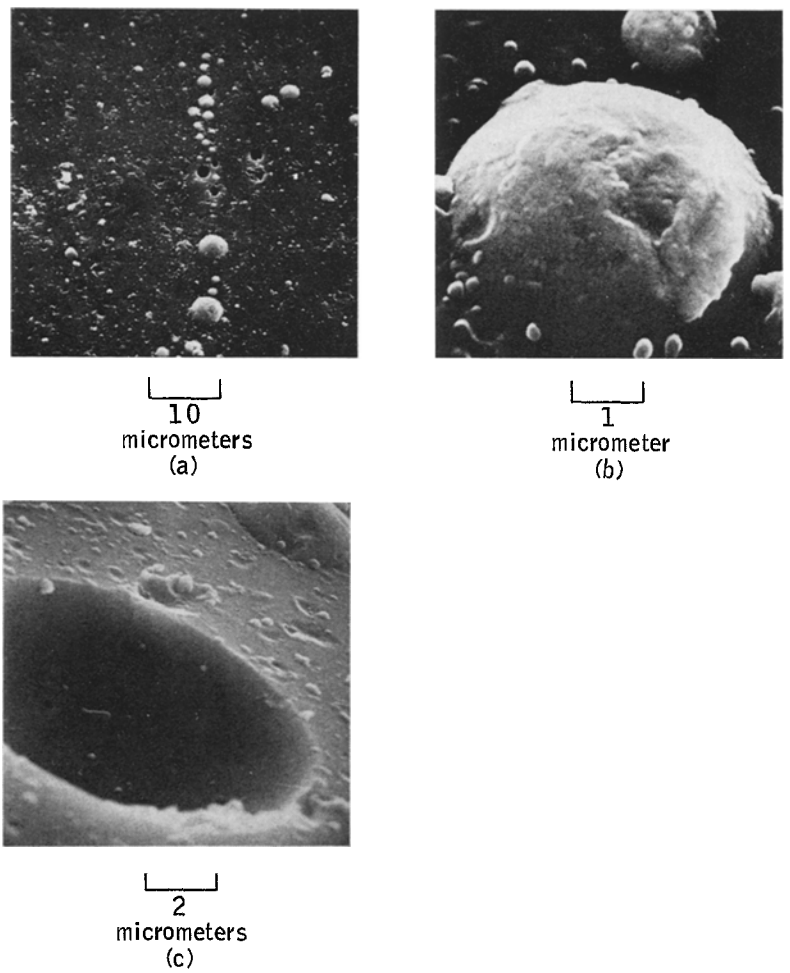

Fig. 3. A group of mounds and dimples on the spherule shown in Figure 1 (a). (a) The dimples are genetically related to the mounds and represent the site where a mound previously existed. (b) Closeup showing mound details. The mound material does not mix with the spherule material. (c) Detailed view of the interior and rim of a dimple. A raised rim or lip and fractures are absent. Note the vesicle inside the dimple. Apparently, the mound material and the spherule were both molten and near molten when the mounds were formed on the spherule.

removal is not understood, but the removal must occur after solidification of the spherule. Suggestions are that the mounds work free because of different thermal-expansion coefficients for the mound and spherule materials or that the stresses produced by subsequent shock waves at the contact between the spherule and the mound cause removal of the mound.

C. STREAKS, RIDGES, AND GROOVES

A number of linear streaks, ridges, or grooves (Figure 4) occur on the surface of the spherule shown in Figure 1(a). It is not always possible to determine whether the features are present in the spherule material itself or in a thin coating of material on the spherule. Closeup examination of these features indicates that the materials involved were viscous fluids at the time of the formation of the features. Radial patterns suggest the possibility that a mixture of melted and solid material collided with the solid spherule, causing part of the melted material to splash onto the spherule and the continued motion of solid material to produce linear features in the melted material coating the spherule surface.

D. ACCRETION PHENOMENA

Angular fragments, vesicular glass coatings, smooth glass coatings, and spheroidal droplets were observed sticking to the spherules (Figure 5). In the case of the angular, solid fragments sticking to the spherules, it is not possible to determine whether the sticking wa scaused by the still hot, and therefore sticky, nature of the spherule or by a small amount of hot, viscous material mixed with angular fragments. Glass coatings clearly flow over and adhere to the surface of the solid spherule. In no case was mixing of the accreted material with the host material observed. Tentatively, it is concluded that most accretion phenomena occur after the host spherule has solidified.

E. IMPACT CRATERS

A population of impact craters (Figure 6) was observed on the spherule shown in Figure 1(b). The following three classes of microcraters have been proposed by McKay (1970) based on the presence or absence of a pit and a spall zone.

Type 1: Craters with pits and concentric spall zone.

Type 2: Craters with spall zone or fracture area only.

Type 3: Craters with pits only.

Craters of each type were also observed on the Luna 16 spherule.

Pits probably are always lined with remelted or remobilized glass. Craters with such pits (Types 1 and 3) are of particular interest. The relationship between these two crater types is illustrated in Figure 6(a) to 6(f). Pit-only craters (Type 3), shown in Figures 6(a) and 6(b), consist of a pit surrounded by a raised rim of material melted or mobilized by the crater-forming impact. The rim material often contains small vesicles. Some rims, possibly those associated with somewhat larger pits, have a concentric but radially discountinuous pattern (Figure 6(c)).

Frequently, somewhat larger pits are partially or wholly surrounded by concentric

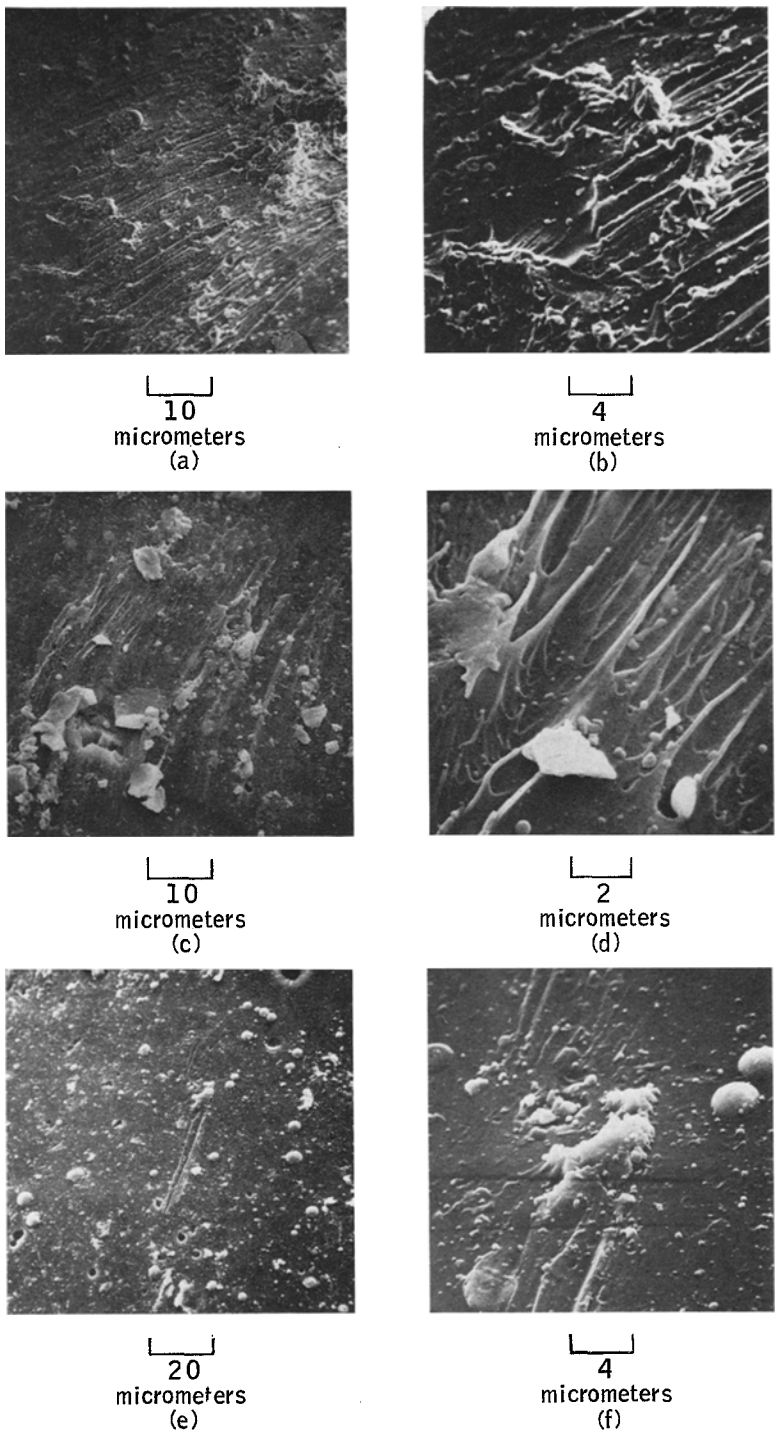

Fig. 4. A variety of grooves and ridges on the spherule shown in Figure 1 (a). (a) A radial pattern emanating from clumps of material to the right of the view. (b) Detail of Figure 4 (a). (c) Streaks of material suggesting flow or motion across the surface of the spherule. (d) Detail of Figure 4 (c). (e) Groove at the center of a typical view of the spherule surface. (f) Detail at the end of the groove showing a clump of material that may have caused the groove.

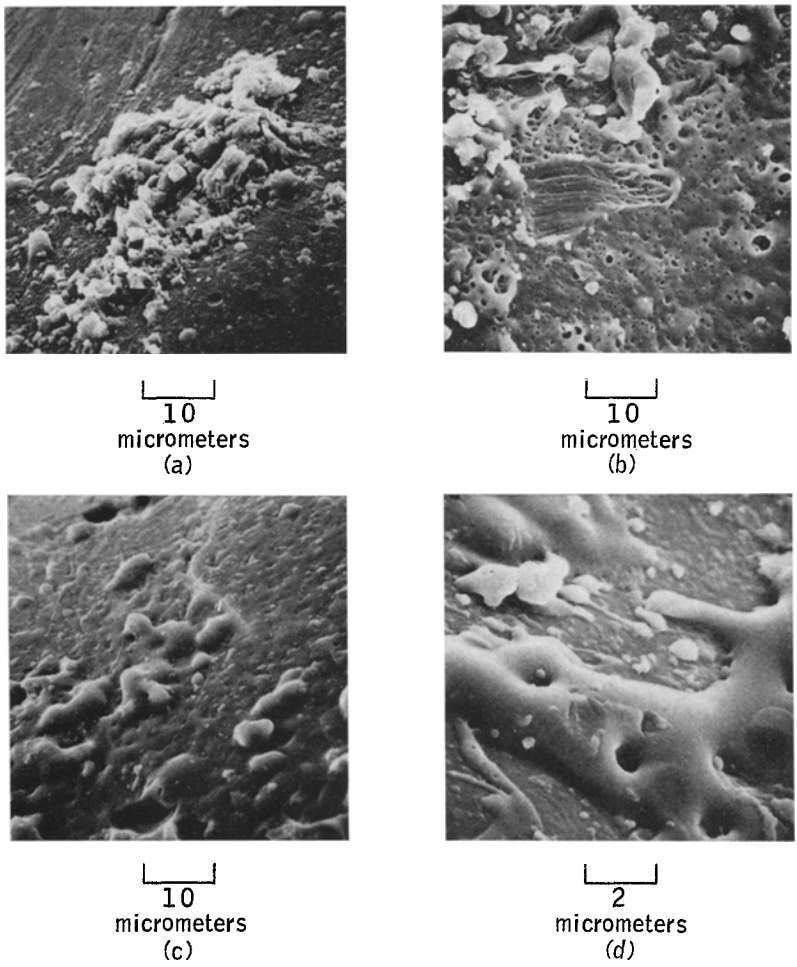

Fig. 5. Different types of material observed sticking to the surface of the spherule shown in Figure 1 (a). (a) Angular fragments may have stuck to the spherule when it was still molten. Alternatively, the sticking may be caused by molten material accompanying the fragments when they encountered the cold spherule. (b) Vesicular glass coating on a part of the spherule. Streaks at the center occurred while the coating was still molten. (c) Nonvesicular glass coating covering sphere and other lumpy material. (d) Detail of contact between spherule and glass coating.

fractures outside the raised rims (Figures 6(c) and 6(d)). These fractures are interpreted as representing incipient spallation. A complete range in the extent of spallation exists, from minor amounts of material removed (Figure 6(d)) to a circular spall zone, except for one segment where the rim is still intact (Figure 6(e)). Still larger pits are surrounded by complete, concentric spall zones (Figure 6(f)). Concentric and radial fracture patterns are characteristic of the spall zones of these Type 1 craters. A tendency exists for larger craters to have relatively larger spall zones; that is, the spall-to-pit-diameter ratio tends to increase with increasing crater size.

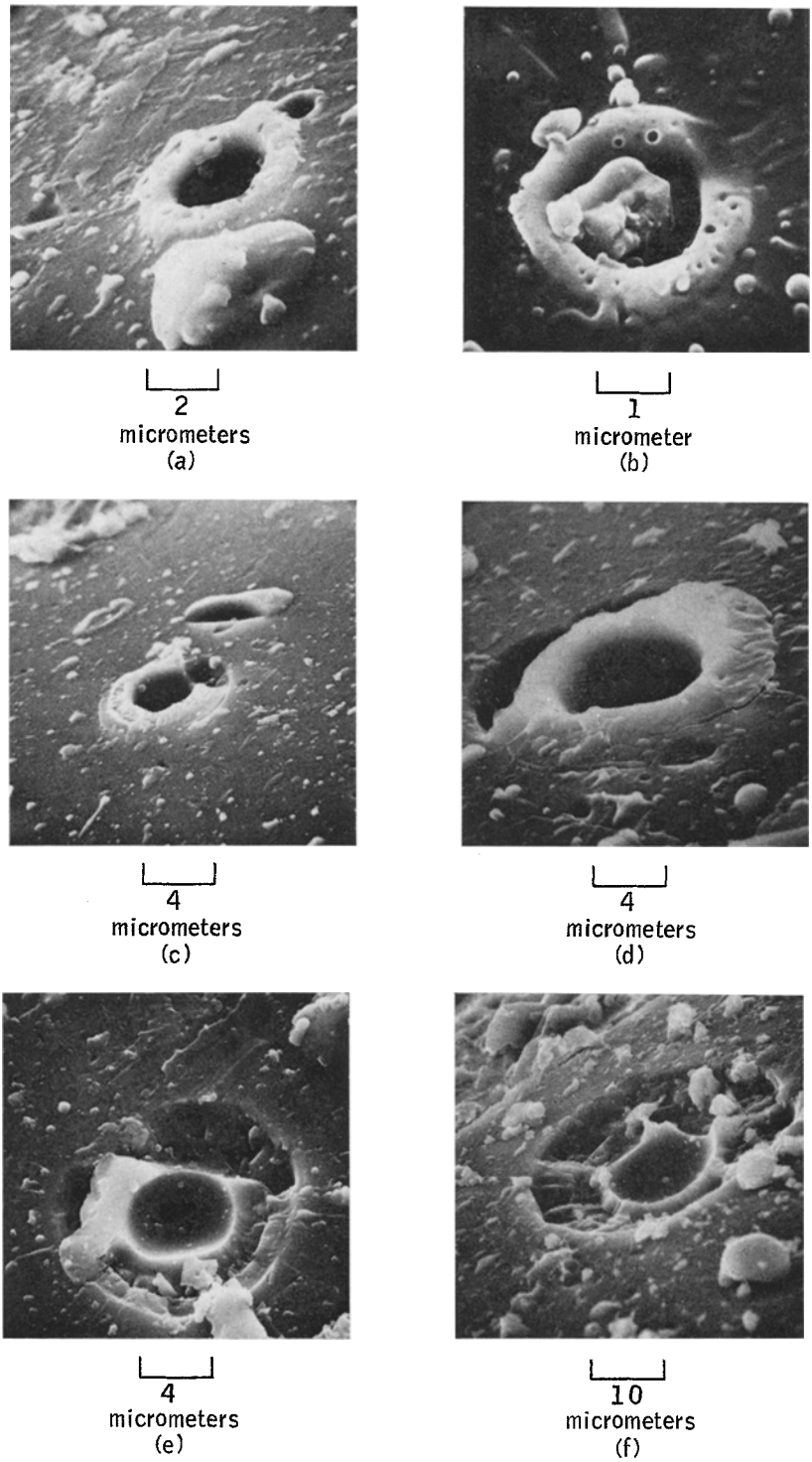

Fig. 6. A variety of high-speed impact craters on the spherule shown in Figure 1 (b). (a) A small crater showing no evidence of related fracturing. (b) A similar crater. Note the raised rim or lip that contains vesicles. The fragment lying within the crater may or may not be related to the formation of the crater. (c) A slightly larger crater surrounded by a concentric fracture. Note the radially discontinuous rim to the left of the pit. (d) A similar, but even larger crater. (e) A small crater with a well-developed spall zone. A portion of the raised rim remains intact. (f) An intermediate-sized crater with a well-developed spall zone that has caused the complete removal of a raised rim. Note the radial and concentric pattern of fractures in the spall zone. The largest crater observed is easily visible in Figure 1 (b).

3. Results of Crater Measurements

Typical microcrater profiles based on parallax measurements of stereoscopic photographs are shown in Figure 7. The relationship between the pit diameter and different

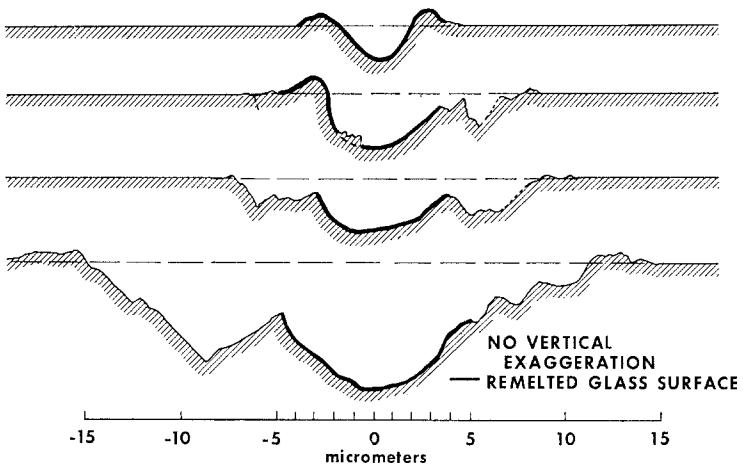

Fig. 7. Typical microcrater cross sections. Transition from pit-only to pit-plus-spall craters and relative increase of spalling effects as crater size increases are shown. Measured cross sections were prepared at the NASA Manned Spacecraft Center Mapping Sciences Laboratory.

types of craters is illustrated further in Figure 8, where the size distributions of different crater types are shown. Measured pit diameters of pit-plus-spall craters are estimated to be approximately 20% low, because a portion of the pit walls is removed by spallation. The conclusions supported by the data shown in Figures 6, 7, and 8 are that crater Types 1 and 3 are transitionally related and that the occurrence of one or the other crater type depends on the pit size, which, in turn, is directly related to the kinetic energy and size of the impacting particle. Laboratory experiments designed to determine quantitatively the relationships described previously are in progress (Vedder, 1971; Mandeville and Vedder, 1971; Bloch *et al.*, 1971b; Carter and McKay, 1971).

The mechanics of spallation or cratering presently are not understood in detail. In general, it is believed that spallation results from tensile failure of the host material in response to stresses produced by the interaction of the impact-produced shock wave with the free surface of the host (Rinehart, 1968). It is known from impact-cratering experiments that the effective strength of the host material increases with decreasing crater size (Gault and Moore, 1965). The relative decrease in the spall-zone diameter with decreasing crater diameter and the complete lack of a spall zone for even smaller craters illustrate and amplify this earlier result. Apparently, the impact-produced tensile stresses present during the formation of pit-only craters are not sufficient to overcome the effective strength of the host material. Another possibility is that, for

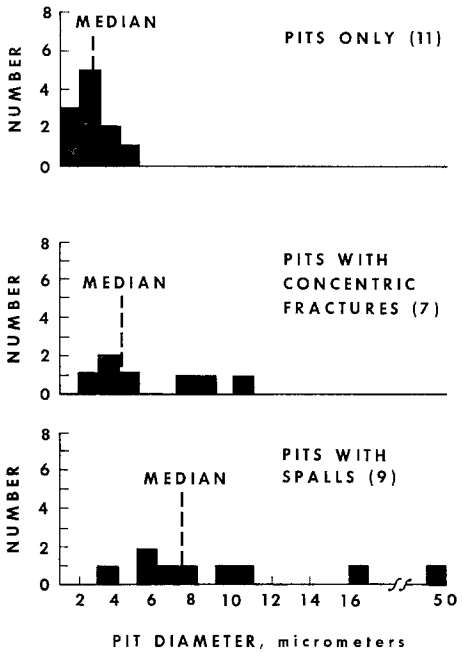

Fig. 8. Size distributions of different types of impact craters. Pit-only craters are generally smaller than pit-plus-spall craters. Intermediate-sized craters that have a pit with a concentric fracture demonstrate the transition between these two crater types. Pits smaller than 1 μm in diameter were not included because these could not be observed quantitatively.

pit-only craters, the duration of the stress pulse is so short that, in effect, a fracture does not have time to form.

A transitional relationship may also exist between pit-plus-spall and spall-only craters (Types 1 and 2). Craters that show no evidence of melting or flow may be attributed to low-velocity impacts incapable of producing shock melts. However, a study of the large pit in Figure 1(b) suggests that the pit may not be attached securely to the spherule. Similar observations were made for larger stylus-pit craters on whole rock surfaces by Hörz *et al.* (1971). Therefore, it is possible that a number of spall-only craters (Type 2) are not produced by low-velocity impact but are caused by high-velocity impacts during which melting occurred. The pits formed may be destroyed or removed either during or sometime after the impact event.

Although the crater types described may appear distinct and well defined, evidence has been presented of gradational transitions from one type to another. Consequently, it is concluded that the various crater types are caused by similar, if not identical, impact processes. Such processes may be either impacts of primary extralunar micrometeorites or impacts of secondary projectiles, that is, ejecta particles set in motion during a somewhat larger impact event. At present, controversy exists regarding which process is reponsible for the crater types observed. An origin by the impact of primary particles is favored for most microcraters on lunar rocks by Hörz *et al.* (1971) and

others, but Carter and McKay (1971) and others suggest an origin by secondary projectiles for micrometer-sized impact features on lunar fines.

A population of 27 microcraters greater than 1 μm in diameter that show evidence of melting or flow related to the impact was observed on the spherule shown in Figure 1(b). For a calculated area of exposure of 0.67 mm^2, the areal density of craters greater than 1 μm is approximately 4000 craters/cm^2. The cumulative areal density or number of craters as a function of pit size is shown in Figure 9.

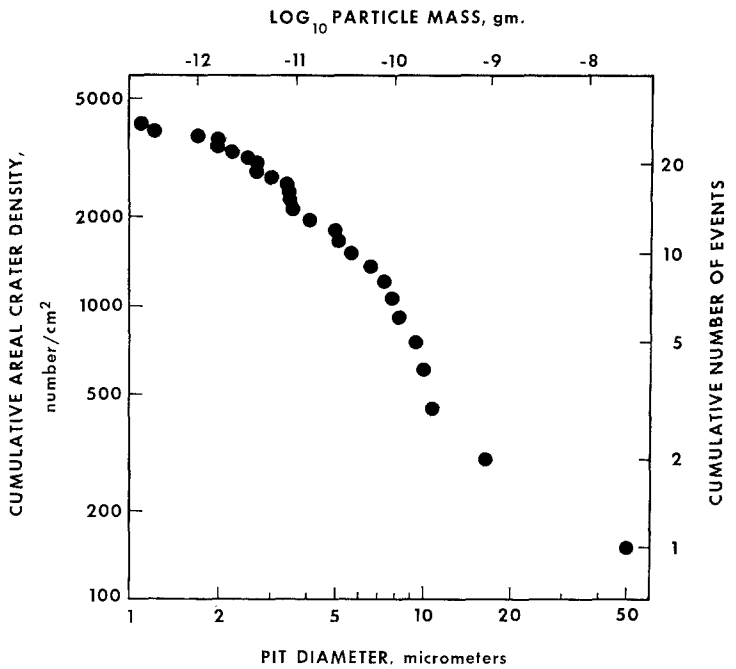

Fig. 9. Integrated areal crater density as a function of crater size. The integrated number of impacting particles as a function of particle mass also shown is based on several assumptions relating the impacting particle and the resulting crater. The $-1/3$ slope of the curve in the 10^{-11} to 10^{-10} g range agrees with values obtained from satelliteborne meteoroid-detection experiments.

Using the hypothesis that the impacting particles were primary, the pit diameters plotted in Figure 9 may be converted into projectile masses. Assuming an impact velocity of 20 km/s, a value of 2 for the ratio of pit to projectile diameter is obtained based on small-scale laboratory cratering experiments (Bloch *et al.*, 1971b; Mandeville and Vedder, 1971). Assuming further, a projectile density of 3 g/cm^3 yields corresponding projectile masses that are included in Figure 9. A slope of approximately $-1/3$ for the log cumulative number as a function of log impacting-particle mass curve is obtained in the 10^{-11} to 10^{-10} g range. This slope is somewhat steeper than those suggested earlier by Bloch *et al.* (1971b), Hörz *et al.* (1971), and Hartung *et al.* (1972), based on optical microscope observations of lunar rock surfaces and preliminary scanning electron microscope observations. However, this value agrees with later

results based on scanning electron microscope observations reported by Fechtig (1972) and remarkably well with an integration of results obtained from satellite-borne experiments designed to measure interplanetary particle flux (Cour-Palais, 1969).

If the microcraters were formed by secondary impacts of lunar particles, then it may be concluded that the size-frequency relationships for secondary craters in this size range are similar to those expected for primary craters.

References

Bloch, M. R., Fechtig, H., Gentner, W., Neukum, G., and Schneider, E.: 1971a, *Proc. Second Lunar Sci. Conf.* **3**, 2639.

Bloch, R., Fechtig, H., Gentner, W., Neukum, G., Schneider, E., and Wirth, H.: 1971b, *Natural and Simulated Impact Phenomena – A Photodocumentation*, Max-Planck-Institut für Kernphysik, Heidelberg, 149 pp.

Carter, J. L. and MacGregor, I. D.: 1970, *Proc. Apollo 11 Lunar Sci. Conf.* **1**, 247.

Carter, J. L. and McKay, D. S.: 1971, *Proc. Second Lunar Sci. Conf.* **3**, 2653.

Cloud, P., Margolis, S. V., Moorman, M., Barker, J. M., Licari, G. R., Krinsley, D., and Barnes, V. E.: 1970, *Proc. Apollo 11 Lunar Sci. Conf.* **2**, 1793.

Cour-Palais, B. G.: 1969, *NASA Space Vehicle Design Criteria – Environment. Meteoroid Environment Model – 1969 (Near Earth to Lunar Surface)*, NASA SP-8013.

Devaney, J. R. and Evans, K.: 1970, *Proc. 28th Annual Mtg. Electron Microscope Soc.*, Claitor's Publ. Div., Baton Rouge, La., 20. p.

Fechtig, H.: 1972, *Proc. Int. Astron. Union Colloq. 13, The Evolutionary and Physical Problems of Meteoroids*, in press.

Frondel, C., Klein, C., Jr., Ito, J., and Drake, J. C.: 1970, *Proc. Apollo 11 Lunar Sci. Conf.* **1**, 445.

Gault, D. E. and Moore, H. J.: 1965, *Scaling Relationships from Microscale to Megascale Impact Craters*, NASA TM-X-54996.

Hartung, J. B., Hörz, F., and Gault, D. E.: 1972, *Proc. International Astron. Union Colloq. 13, The Evolutionary and Physical Problems of Meteoroids*, in press.

Hörz, F., Hartung, J. B., and Gault, D. E.: 1971, *J. Geophys, Res.* **76**, 5770.

Mandeville, J. C. and Vedder, J. F.: 1971, *Earth Planetary Sci. Letters* **11**, 297.

McKay, D. S.: 1970, *Proc. 28th Annual Mtg. Electron Microscope Soc.*, Claitor's Publ. Div., Baton Rouge, La., p. 22.

McKay, D. S., Greenwood, W. R., and Morrison, D. A.: 1970, *Proc. Apollo 11 Lunar Sci. Conf.* **1**, 673.

Neukum, G., Mehl, A., Fechtig, H., and Zähringer, J.: 1970, *Earth Planetary Sci. Letters* **8**, 31.

Rinehart, J. S.: 1968, in *Shock Metamorphism of Natural Materials*, Mono Book Corp., Baltimore. Md., p. 31.

Vedder, J. F.: 1971, *Earth Planetary Sci. Letters* **11**, 29.